Systematic Study of the Taylor Method for Production of Cu-based Shape Memory Alloy Microwires

A Master's Thesis by

Eric Szablinski

B.S. Material Science and Engineering
University of Arizona, 2010

SUBMITTED TO THE DEPARTMENT OF MATERIAL SCIENCE AND ENGINEERING IN PARTIAL FULFILLMENT OF THE REQUIREMENTS FOR THE DEGREE OF

MASTER OF SCIENCE IN MATERIAL SCIENCE AND ENGINEERING
AT THE
MASSACHUSETTS INSTITUTE OF TECHNOLOGY

September 2012

Author.....
Department of Material Science and Engineering
July 2nd, 2012

Certified by.....
Christopher A. Schuh
Department Head, Material Science and Engineering
Thesis Advisor

Accepted by.....
Gerbrand Ceder
Chair, Departmental Committee on Graduate Students

Systematic Study of the Taylor Method for Production of Cu-based Shape Memory Alloy Microwires

A Master's Thesis by

Eric Szablinski

Submitted to the Department of Materials Science and Engineering on July 6, 2012 in partial fulfillment of the requirements of the Degree of Master of Science in Material Science and Engineering

Abstract:

The Taylor method is a proven way to produce Cu-based shape memory microwires that aren't plagued by problems typical in polycrystalline copper SMAs produced by other methods. Here we set out to expand and refine this processing method to take the first critical steps toward large-scale continuous production. Using a semi-automated processing route, we draw continuous, uniform fibers up to 5 meters in length with diameters in the range 10 - 35 microns. Particular attention is paid to microwires made from a Cu-Sn shape memory alloy. In addition, because the properties of shape memory microwires depend on their diameter, processing parameters were varied to understand their impact on the diameters of the resulting wires.

Thesis Supervisor: Chris Schuh

Title: Department Head, Material Science and Engineering

Acknowledgements:

I'd like to thank my mom, dad, and sister whose endless support led me to where I am today. Next, I'd like to thank Chris Schuh for believing in me, even when I didn't. I'd also like to thank everyone in the Schuh Group, and Stian in particular, for offering ideas and guidance for these last few years. I'd like to thank my friends for reminding me that I'm not alone. I also offer my gratitude to the army for providing funding.

Finally, I'd like to thank my roommate Devin, for cooking spaghetti.

Table of Contents:

List of Figures:

List of Tables:

1. Introduction:

Shape memory alloys are magic. Or, at least, that is how it might appear at first glance. A spring, for instance, made from this amazing metal can be bent out of shape and then placed over a flame. Once heated, the bent wire can, with no other forces applied, curl itself back up and return to its original form: a spring. This is an example of the shape memory effect.

This "magic" metal, this shape memory alloy (SMA), is able to do this because of an interesting diffusionless solid-state phase change known as a martensitic transformation. Not only does martensitic transformation give rise to the shape memory effect (SME), it can also give rise to a second unusual property known as pseudoelasticity. Pseudoelasticity is the property that allows recoverable strain in alloys far beyond that of typical metals. Typical strains of 2% to 6% are often achieved [1-6], and in some cases, recoverable strains of up to 12% are possible [7]. The SME, on the other hand, allows an alloy to recover its original shape after deformation through the application of heating.

Nickel Titanium (Nitinol) is currently the most common and well-known SMA [2, 4-5, 8-11]. Nitinol springs are commercially being used in a variety of applications such as eyeglass frames [4], orthodontic wire [8], and mobile phone antennae [9]. The most prevalent uses of Nitinol, however, are in fields where cost is not a prohibiting factor such as in the aerospace and the medical industries. SMAs have been used as hydraulic guide wires for catheters [4], stents [9], couplings for the F-14 [10], and in a porous form

have been used to assist bone repair [5, 8]. The main drawback to Nitinol is price. Not only are the materials expensive, but processing Nitinol so that it will exhibit SME or pseudoelasticity also drives up the cost [11]. Cu-based alloys, on the other hand, offer an attractive alternative due to their reduced material cost, and potentially equally versatile shape memory properties.

There are a variety of copper alloys that can be used as SMAs. Many could be made for only a fraction of the cost of traditional Nitinol alloys, but most aren't commercially available yet due to problems that arise in copper systems, such as intergranular fracture and poor fatigue life. Copper systems have a much higher elastic anisotropy than their nickel titanium counterparts, leading to much higher stresses at grain boundaries, particularly at triple junctions [2, 10-11]. These stresses lead to fractures at the grain boundaries that drastically reduce the fatigue life, or may even prevent the appearance of the SME at all [2, 11-12].

One method to solve this problem is to eliminate triple junctions altogether. By creating thin, micron-sized fibers it is possible to grow grains that extend through the entire diameter of the fiber. Then all that remains are grains that take on a "bamboo-like", or oligocrystalline structure, where all grain boundaries are perpendicular to the wire axis and are adjacent to only two grains. These microwires can, and have been successfully produced by a process known as the Taylor method. The Taylor method, put simply, is a process of drawing liquid metal through a glass capillary.

Several metals and alloys have been successfully drawn by the Taylor method including a few SMAs [1-2, 13], but there is little data regarding how altering the processing parameters affects the diameters of the wires produced. In addition, the SMAs drawn by this process have only been short lengths, drawn by hand, and often of variable quality [2]. A more continuous and reproducible, mechanical method must be developed if there is any hope of employing these microwires on a large or industrial scale.

The purpose of this thesis is as follows:

- To develop and demonstrate a semi-automated version of the Taylor method processing route to draw continuous, uniform wires on a meter length scale.
- To systematically examine how differing the processing parameters affect the resulting properties of the wires produced.
- Finally, to use this method to attempt to draw microwires with shape memory properties.

2. Background:

2.1 Shape Memory Alloys:

Shape memory alloys (SMAs) exhibit a number of interesting properties that could be useful in applications such as actuation, sensing and damping. These properties arise from a diffusionless phase change known as a martensitic transformation. At low

temperature and/or high stress conditions, a SMA will be in a twinned or detwinned martensitic phase, while at high temperatures it will be in an austenitic or parent phase.

2.1.1 Mechanistic Origins of Shape Memory Properties

In an alloy that exhibits the shape memory effect (SME), the alloy begins in the low temperature, twinned martensite phase. The typical thermomechanical cycling of SME materials is shown by the orange arrows in Figure 1. Stress is applied causing the martensite to de-twin, resulting in a visible, macroscopic change in the shape of the piece. Then the temperature is raised, transforming the alloys into the parent phase. When the part is cooled, it will revert back to the twinned martensite phase, recovering its original shape.

SMAs can also exhibit pseudoelasticity, or superelasticity as it is sometimes called. In this case, the alloy begins in the high temperature parent phase, as shown by the blue curve in Figure 1. Stress is applied causing the nucleation of a detwinned martensite. When the stress is unloaded, the alloy reverts back to its parent phase. Pseudoelasticity can therefore be used to achieve strains in metal far beyond that of typical alloys.

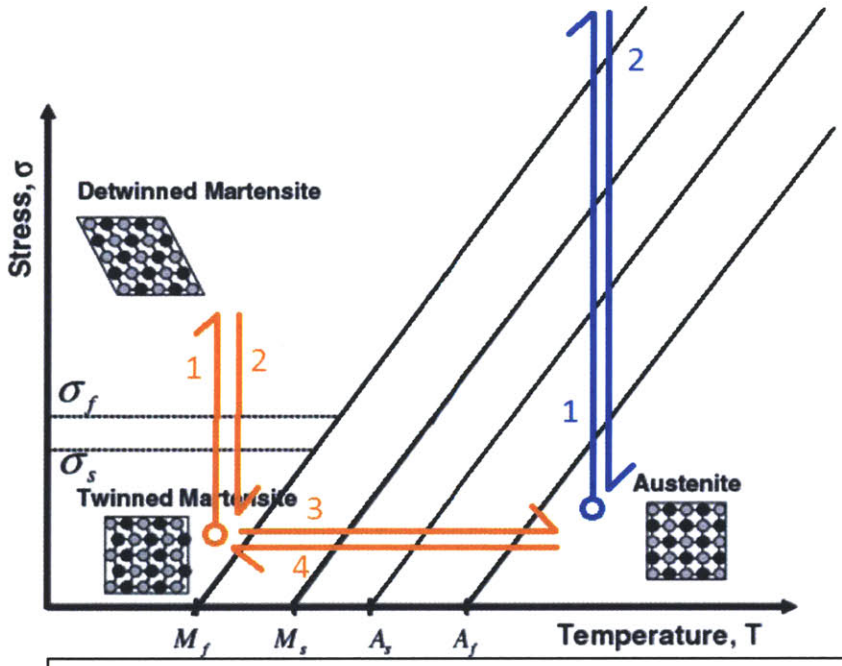

Figure 1. A schematic phase diagram of a shape memory alloy (SMA). Typical thermomechanical cycles are shown: pseudoelasticity (blue) and the shape memory effect (orange)
Adapted from source [10]

It is important to note that that these phase changes don't occur instantaneously. When temperature is lowered M_s corresponds to the temperature where martensite starts to form, and M_f corresponds to the temperature where martensite finishes forming. Likewise, when the temperature is raised A_s and A_f are the temperatures known as the austenite start and austenite finish, respectively. Similarly, σ_{Ms}, σ_{Mf}, σ_{As}, and σ_{Af} are the stresses where each phase starts and finishes forming. These stresses and temperatures are unique from each other. This causes hysteresis to appear when the alloy is thermomechanically cycled, leading to a net dissipation of energy.

2.1.2 Useful Applications

There are many potential applications for shape memory alloys that would utilize both the SME and its pseudoelastic properties. Microwires, in particular, would be useful if combined to form braids, cables, or fabrics.

One potential application is damping. Under pseudoelastic cycling, there will be hysteresis in the stress-strain curve due to differences in σ_{Ms}, and σ_{As}. The area enclosed in this hysteresis loop is equal to the energy dissipated, or damped, in a single cycle. The specific damping capacity for SMAs is higher than most known materials [13]. This makes SMAs ideal materials for vibration reduction, and impact absorption.

The shape memory effect could also be useful if applied to fabrics. Current work being done at MIT [14] is looking into making textiles from shape memory fibers for use in spacesuits. Astronauts need pressure on their skin in order to survive in space. This problem is currently solved by pressurizing the suit with air. This solution, however, severely limits their mobility, as every movement requires pushing against all the air in the suit. Tight fitting suits could also provide the necessary pressure, but they are nearly impossible to get on. Active materials, like SMAs, might hold a solution. They can go on loose, and then can apply the pressure to the skin when properly activated.

2.1.3 Cu-based SMAs

Cu-based SMAs offer an economic alternative to traditional nickel titanium alloys, and could hold the key to wider adoption of SMAs beyond aerospace and

biomedical applications. There are a number of copper alloys with excellent shape memory properties including: Cu-Al-Ni [13, 15], Cu-Al-Zn [16], Cu-Al-Mn [17], Cu-Zn [6], Cu-Zn-X (with X being a number of transition metals) [18-19], and Cu-Sn [20-21]. In their single-crystalline forms Cu-based alloys have properties that rival those of current Nitinol alloys. Problems arise in their polycrystalline forms. High elastic anisotropy causes high stresses to occur at grain boundaries due to incompatibilities during phase transformations [2, 10-11]. This leads to intergranular fracture which dramatically reduces the fatigue life to a few cycles [2, 11-12].

Transformation temperatures of these alloys range from -100 to 150 °C and are largely dependent on composition [21-22]. Recoverable strains of 12% have been achieved with these alloys [7]. Specific Cu-based systems can also offer a wide range of other useful properties such as biocompatibility and corrosion resistance [23], as well as high electrical and thermal conduction. Cu-based SMAs would be suitable for a broad range of applications and environments.

2.2 The Taylor Method:

The Taylor method is a processing route that draws wires directly from the melt. It was originally pioneered by Taylor in 1924 as a method for producing fine diameter wires for use in thermocouples and resistive thermometers [24]. The original method involved two steps. The first step involved heating a small piece of metal inside glass tubing (with one end closed), removing any oxidation or slag with forceps and drawing the metal into one foot lengths approximately a millimeter in diameter. These glass

coated metal filaments could be drawn into high quality microwires by passing them through heated cylinders of appropriate size [24]. This method of drawing microwires directly from the melt was a more economical solution than previous microwire forming processes which required forcing solid wire through successively smaller dies to produce finer and finer wires [25]. Taylor was able to successfully draw many metals including copper, tin, antimony, lead, bismuth, iron, gallium, and aluminum among others [24]. The Taylor method, however, lied fallow for a couple decades because there was little need for fibers that thin and they were mostly thought of as lab curiosities [25].

This process relies on the fluidic properties of glass. When heated, glass doesn't just melt, like most materials. Glass softens. The viscosity of glass follows an Arrhenius curve and decreases continuously as temperature is increased allowing it to be worked and formed. The temperature at this point is colloquially known as the "working point" and corresponds to the temperature where the viscosity of glass equals 10^3 Pa*s. If the working point of the glass is between the melting and boiling point of the metal, and the metal doesn't react chemically with the glass, microwires of diameters from 1 – 100 microns can readily be obtained [24-30]. The softened glass provides support and protection to the molten metal core during the draw, which ultimately is why the metal can be drawn in wire form at all.

The process began to regain popularity in the 1960's and interest continues to the present day [25-33]. The Taylor method has been looked at for its potential use for filters [25], composites [26], electronics [27], sensors [28], amorphous metals [29-31], and most

recently, for shape memory materials [1-2, 31-32]. The process has been refined since its introduction into a single step. Metal is placed inside a glass tube that is closed at one end and heating is applied (usually by induction furnace) until the metal melts and the glass softens. The glass is then drawn directly into a microwire by spooling the fiber onto a rotating take-up drum. The glass can then be removed with a solution of HF, or by mechanically breaking the glass from the surface by pinching the microwire between two plates.

The diameter of fibers made by this process have been controlled in multiple ways. Baikov [34] reported that the diameter could be varied by adjusting the take-up speed and cooling rate. McKenica [35] stated that diameter was affected by the diameter of the initial glass tube, take-up rate, feed rate, and overall temperature [35]. Others have reported that diameter is dependent on draw speed [26], temperature [26-27] cooling [27-28], but actual data is sparse, and may be specific to the individual apparatus used in each experiment.

2.3 Shape Memory Microwires:

Diameter is a particularly important feature in SMA microwires because the properties are dependent on size [1-2]. In particular, the size of a SMA affects the size of the stress hysteresis, which in turn will determine the specific damping of the material. Chen [1] made microwires of a Cu-Al-Ni alloy using a hand-pulled version of the Taylor method. She found that as the diameter of the wires decreased, $\Delta\sigma$ (defined as $\sigma_{Ms} - \sigma_{As}$), increased. This means that the stress hysteresis was larger in microwires with finer

diameters. Ueland added further evidence for this trend by making microwires of a Cu-Zn-Al alloy. He showed that this size effect was not unique to a single alloy. Further, he was able to show that his oligocrystalline microwires showed fatigue strength on par with single crystalline SMA of the same alloy, as well industrial standard Nitinol alloys.

3. Experimental:

Alloys of nominal compositions of Cu-15at%Sn and Cu-40at%Zn were prepared by melting appropriate amounts of elemental powders in quartz ampules under argon. These alloys were chosen primarily because tin, in particular, was noted to work well with the Taylor method [24], and Cu-Zn was chosen as a simple alloy for comparison. The compositions were then verified using energy dispersive spectroscopy (EDS). Several samples were also subjected to wet chemical analysis (at Dirats Laboratories, Westfield, MA) to further verify compositions and validate the EDS results.

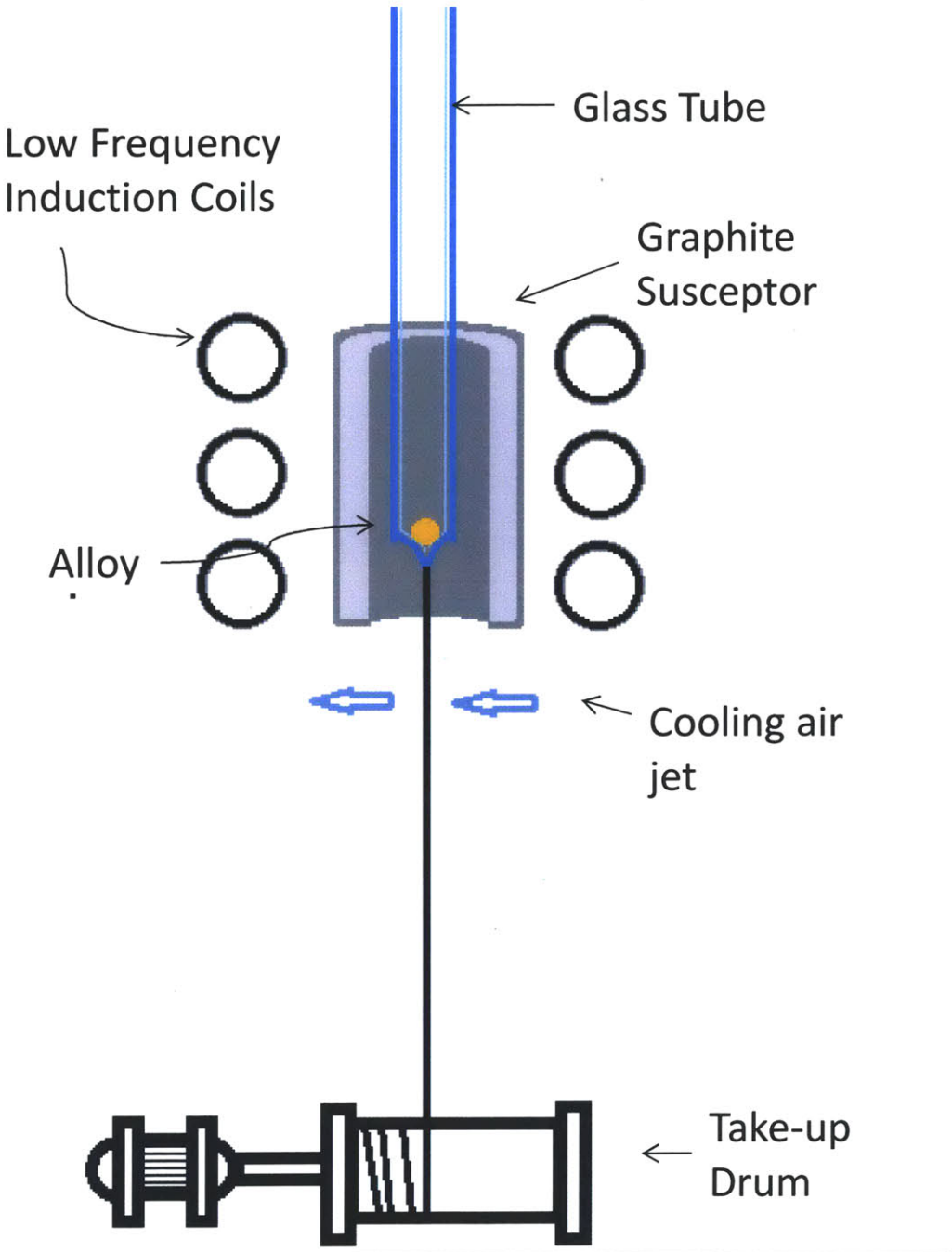

Figure 2. A schematic drawing of the Taylor method drawing machine

Wires were drawn by the Taylor Method using an apparatus schematized in Figure 2. The glass tubing used was a borosilicate glass with a 4 mm inner diameter and 6 mm outer diameter. One end of the glass tube was sealed with a hydrogen flame and a nickel-chrome wire was inserted to facilitate pulling. A low frequency induction furnace was used to heat a cylindrical SiC-coated graphite susceptor to melt the metal and glass. The glass tube was also placed inside a quartz tube with a tapered end in the furnace to provide support when the inner tube began to melt. The fibers were cooled with a jet of air placed approximately 8 cm below the furnace. The fibers were pulled on a winding drum that was capable of lateral motion. The wires were drawn at speeds between 0.1 m/s

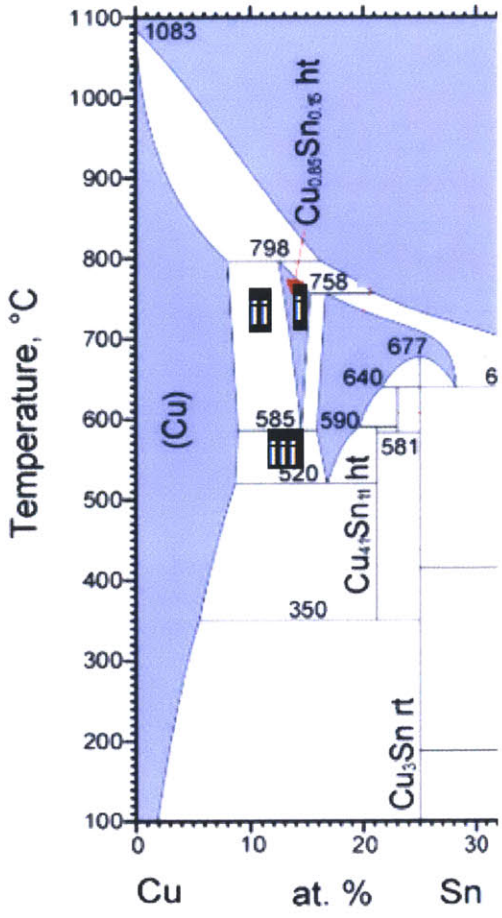

Figure 3. A partial phase diagram of the Cu-Sn system. (i) The superelastic β phase. (ii –iii) Other regions of interest to this study

and 1 m/s. The microwires were then annealed between 700 °C and 750 °C between 15 – 120 minutes to encourage grain growth and solutionize in the β phase shown in Figure 3(i). Wires drawn with this method can be seen in Figure 4 and Figure 5. The glass coating was then removed either chemically, by soaking the fibers in a 5% HF bath overnight, or mechanically, by squeezing the fibers between two plates.

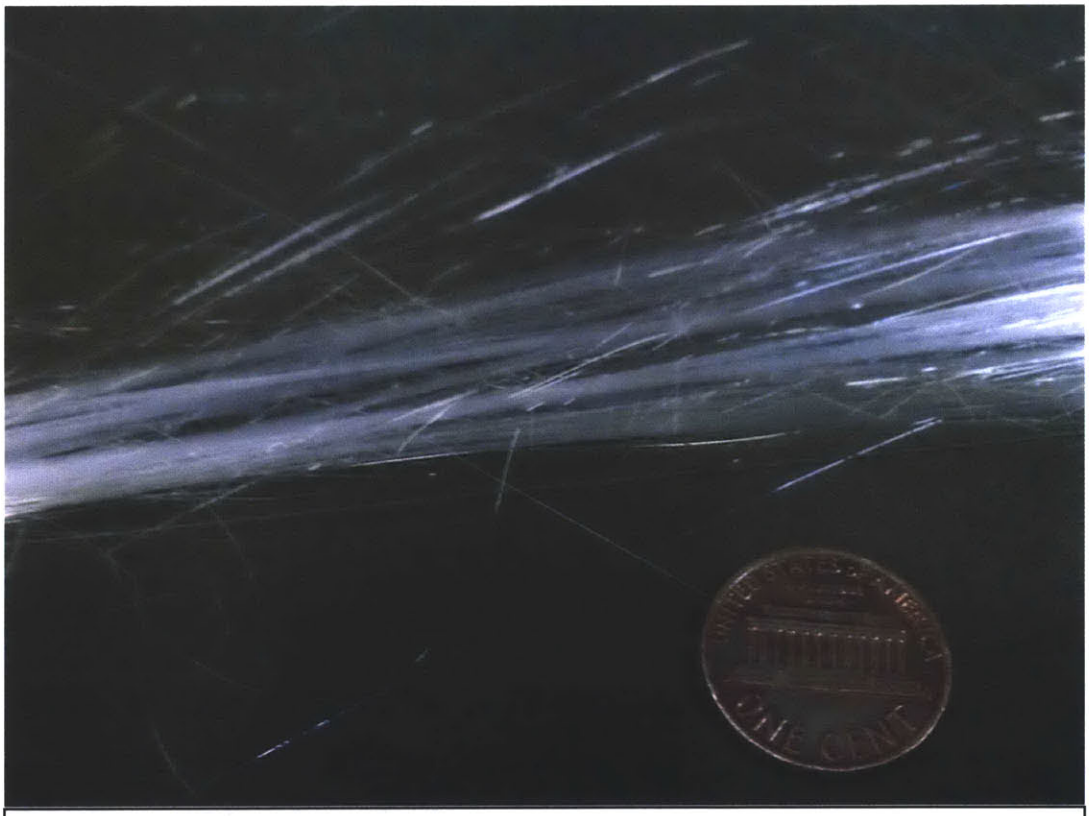

Figure 4. Samples of glass coated microwires.

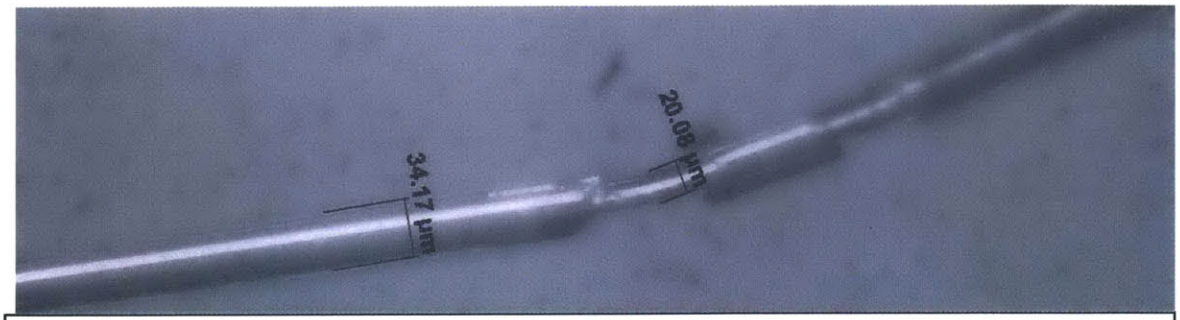

Figure 5. Optical micrograph of microwire with and without its glass coating

4. Variation in Diameter:

A list of microwires drawn at various compositions, draw speeds, and temperatures can be found in the appendix.

Using the apparatus shown above, multiple wires, several meters in length were able to be drawn. Drawing 2 to 4 meters of metal fiber was common. The longest microwire drawn was just a little less than 5 meters.

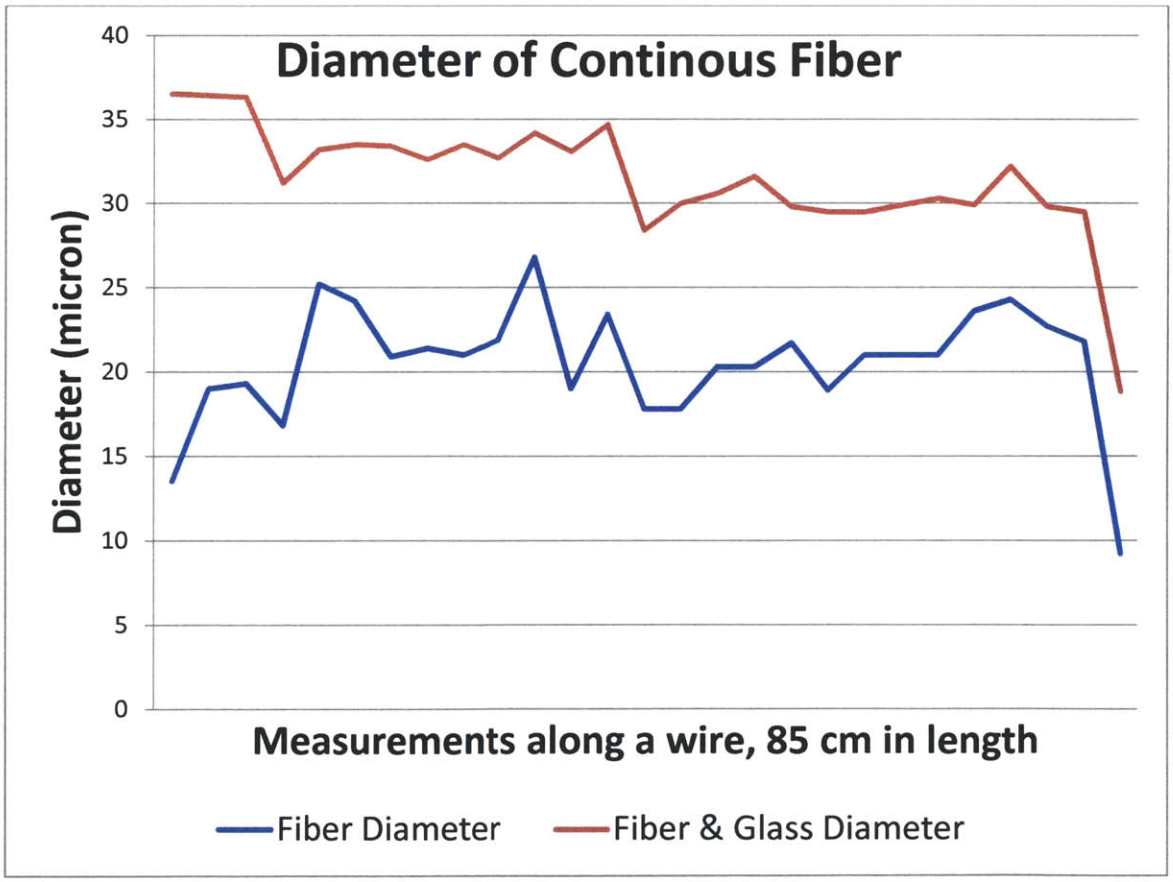

Figure 6. Measurements of the diameter along a continuous section of fiber #50

The lengths of the drawn fibers are ultimately limited by the amount of alloy (about 20mg) placed in the glass tubes to be drawn. No more metal was added during the melt.

Though this is the upper limit, it was not uncommon for the fiber to break partway through the draw. This breakage was attributed to either oxidation, especially for fibers drawn in air, or to surface flaws that developed on the glass sheath during the draw.

The fibers were mostly continuous and few, if any, breaks were observerd along their lengths. In addition, the fibers were nearly uniform in diameter. The diameter of a section of Fiber #50 was measured along its length and a graph of the results is shown in Figure 6. Excluding the ends of the section of wire associated with start-up and ending transients, the average diameter was 21.2 microns, and was uniform in diameter to within 5 microns.

4.1 Effect of Draw Rate:

Fibers were drawn at rates from 0.1 to 1 m/s at temperatures between 1250°C and 1450 °C. The results are shown in Figure 7 and Figure 8. There is a slight decrease in diameter with increasing draw rate. The large spread to the data, however, indicates that there are other factors at play. If we look specifically at Cu-14.5at% Sn we can see the downward trend much more clearly than several other samples. In fact, Cu-15at% Sn and Cu-40at% Zn appear to show the opposite effect over the same range. In total, the speed at which the fibers are drawn has a small effect on the diameters of the resulting fibers.

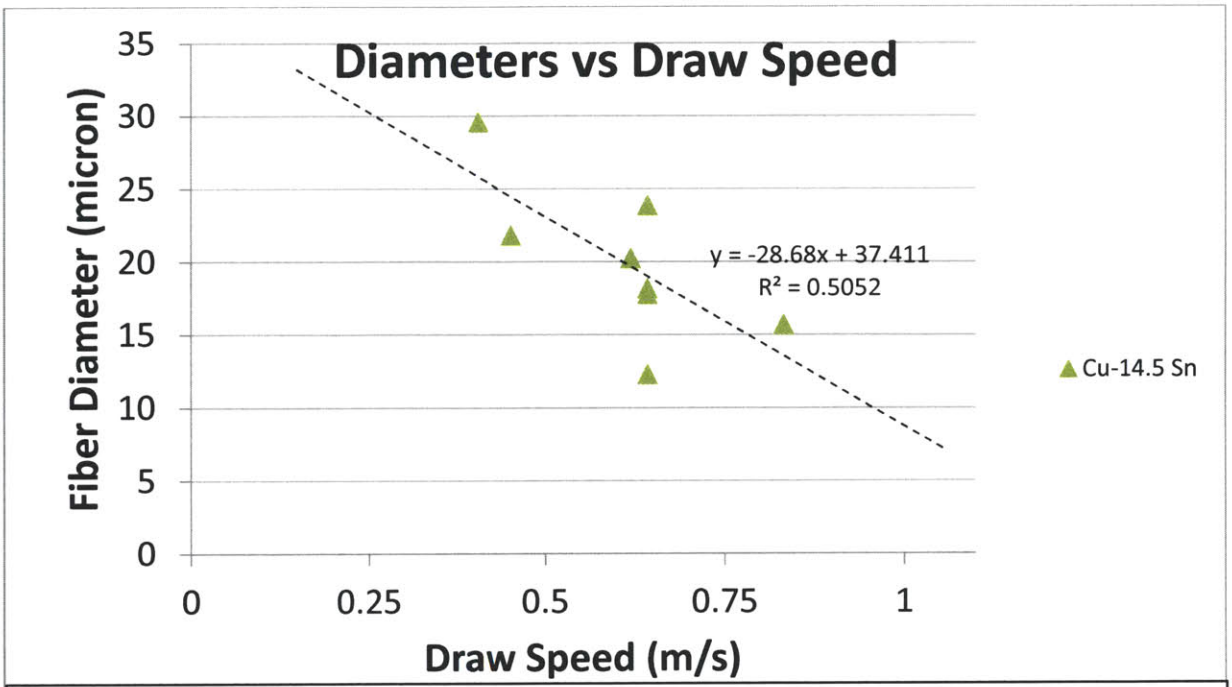

Figure 7. Measurements of fibers #28 – 35 to attempt to determine how diameter is affected by draw speed

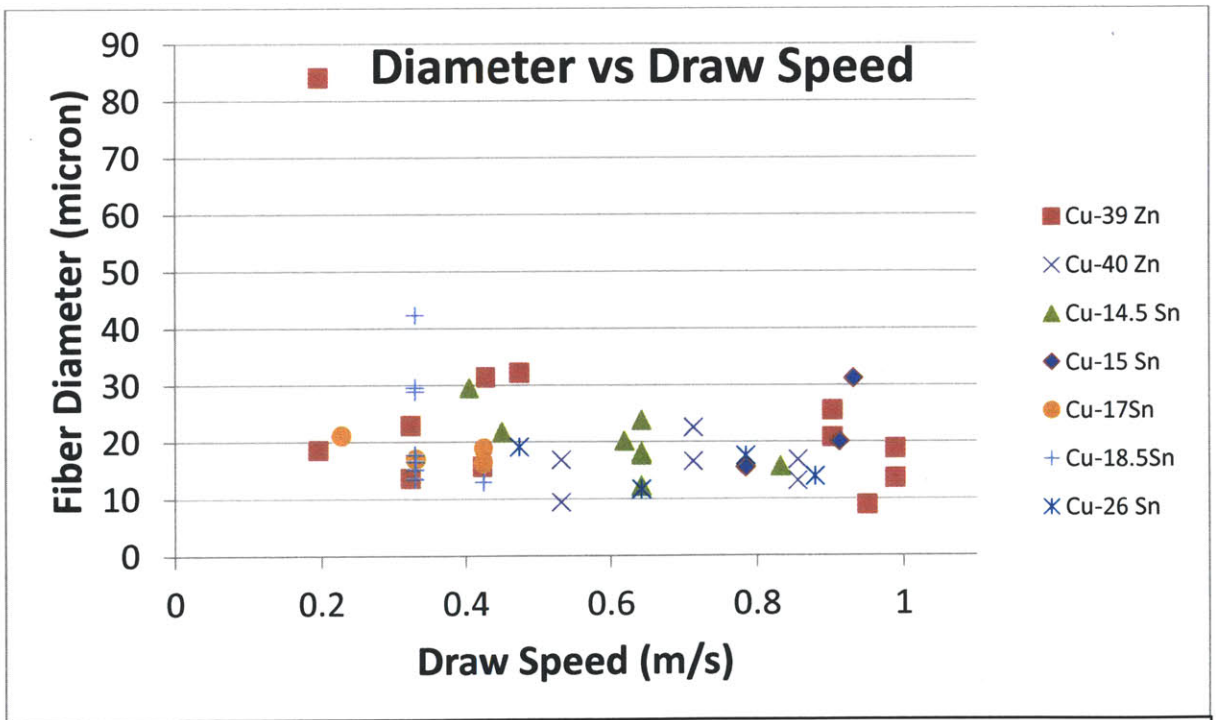

Figure 8. Diameter as a function of draw speed for multiple alloys. No significant trend is apparent from 0.1 to 1 m/s

4.2 Compositional Effects:

Multiple alloys of Cu-Sn and Cu-Zn were produced at slightly different ratios, to test if composition affected the diameters of the wires drawn. Wires were drawn between 1250 –1450 °C at varying speeds. Small changes in composition, as shown in Figure 8 appeared to have no effect on the diameters of the resulting fibers. In fact, Cu-Sn and Cu-Zn alloys have similar diameters regardless of composition.

4.3 Effects of Temperature:

Samples of Cu-17at%Sn were drawn at 32 cm/s. The temperature was measured by placing a bare-metal Type R thermocouple directly into the furnace (the thermocouple didn't self-heat because the induction furnace was a low-frequency furnace, rather than a high-frequency one). Figure 9 shows a clear negative trend. As the temperature is increased, the fiber diameter decreases.

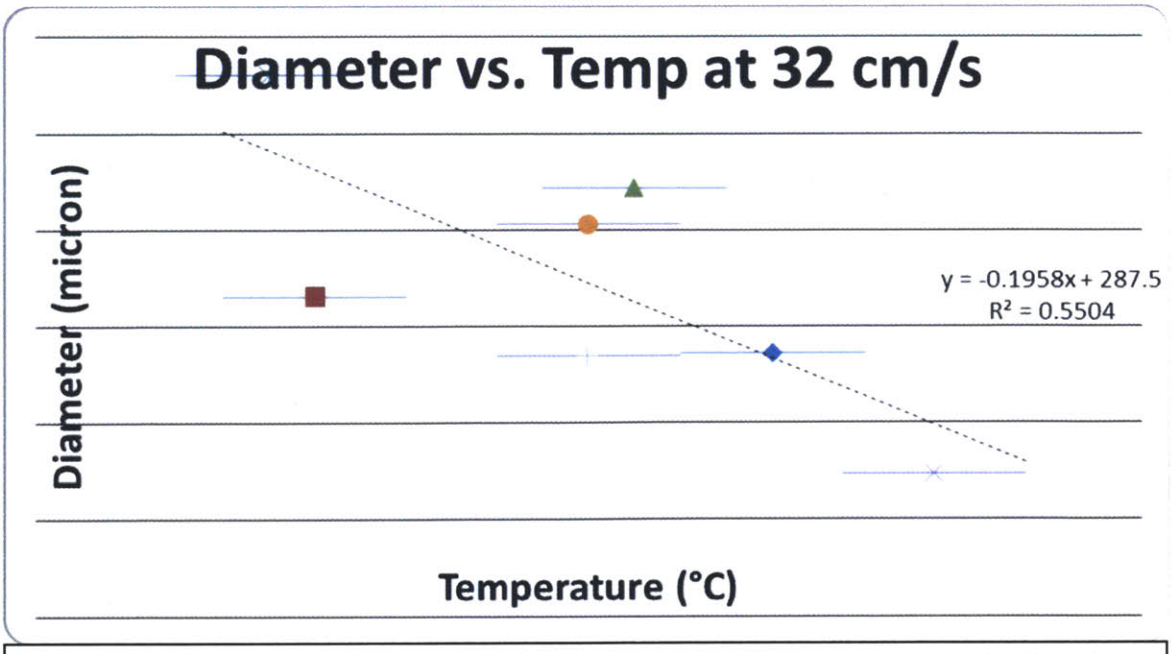

Figure 9. Diameter measurements taken of Wires #62-70 drawn at 0.32 m/s plotted as a function of temperature

This trend can be attributed to the large dependence glass viscosity has on temperature. Over this range of temperatures the viscosity of the glass decreases by nearly an order of magnitude [36]. This decrease in diameter is from 30 μm to 7 μm is nearly identically to the spread of diameters we see in Figure 8. From this, we can infer that it is the properties of the glass that predominantly control the diameter of the fibers, not the composition of the metal. Temperature has a large effect on diameter because of the relatively large change in viscosity, compared to the relatively small change in draw speed.

5. Testing:

An alloy of composition Cu-14.5at% Sn was made by the method previously

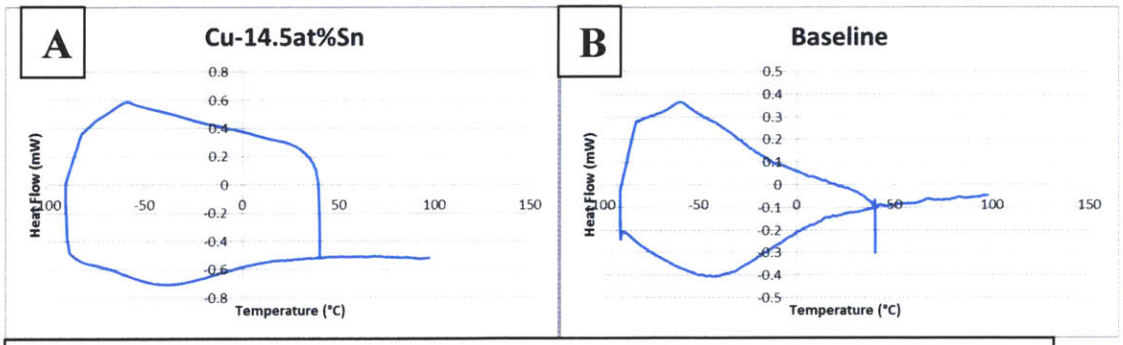

Figure 10. (a) DSC results of tested microwire. There appear to be peaks at -60°C and -35°C (b) Baseline showing the same peaks, meaning the results in (a) are unlikely to be real

mentioned, and the composition was verified by wet chemical testing. Fibers were drawn from this alloy (Fibers #28-#35) and annealed at 750 °C for 60 minutes to promote grain growth and attain the necessary β phase. They were examined using differential scanning calorimetry (DSC) to seek the martensitic transformation on cooling and austenite

reversion on heating. These fibers were expected to have an M_s temperature around -50 °C [3, 7, 37], but Figure 10 shows no significant change from the baseline, indicating that there is no phase transformation present.

To understand why the fibers showed no phase transformation, they were then examined using a scanning electron microscope (SEM) with an attached Energy Dispersive Spectrometer (EDS). The SEM micrograph with the associated EDS analysis is shown in Figure 11. As seen in Figure 11(b) the fiber is purely Cu & Sn, and it doesn't appear that the fiber has picked up any impurities from the glass or any other sources during processing. The quantitative analysis, shown in Figure 11(c), however reveals that fiber has too little tin. Therefore, the superelastic β phase is not present.

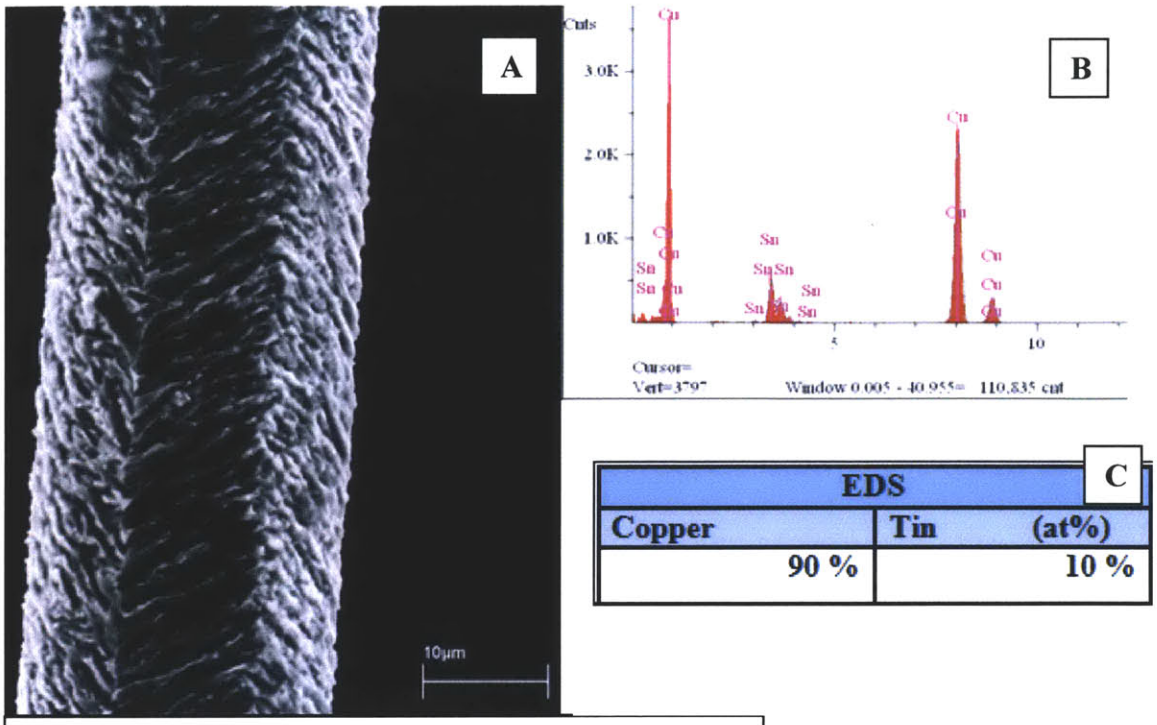

Figure 11. (a) SEM micrograph of wire #34. (b-c) EDS analysis of wire

An alloy of slightly higher tin content, Cu-17at%Sn, was drawn and annealed. As seen in Figure 12, these fibers did not develop an oligocrystalline structure, but are microcrystalline. The backscatter micrograph shows that there are two phases present. These phases contain 10 at% and 15 at% Sn, respectively. This means that the alloy is in the two-phase region of the phase diagram (Figure 3(ii)), and thus, still too low in tin.

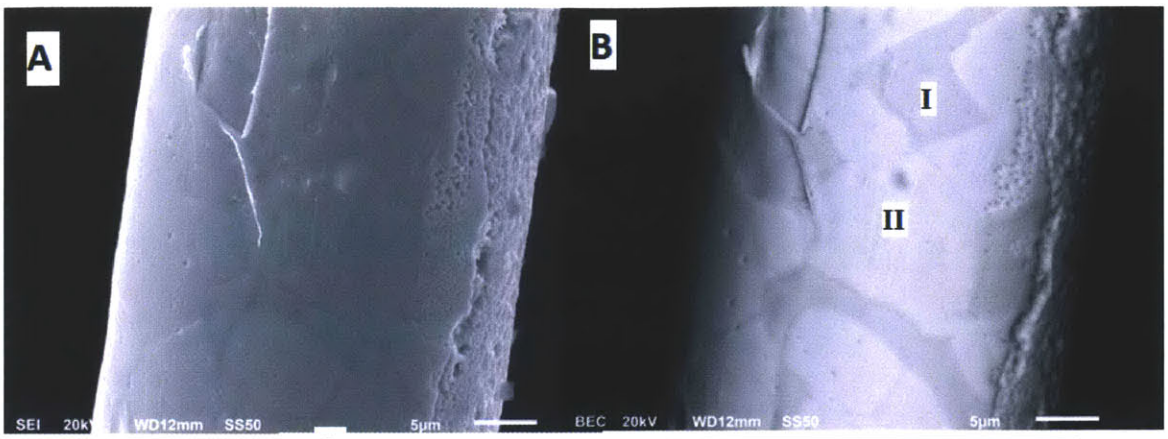

C

EDS Region I		
Copper	Tin	(at%)
91 %	9 %	

D

EDS Region II		
Copper	Tin	(at%)
85 %	15 %	

Figure 12. (a) SEM micrograph of wire #65. Annealed at 750 °C for 15 minutes and quenched in ice brine. Glass coating removed mechanically. (b) Same image viewed in backscattered mode to show compositional contrast. (c-d) Quantitative EDS results of Regions I & II

These low tin concentrations in the fibers are thought to be a result of differences in vapor pressure and loss due to volatilization. As seen in Table 1 at relevant temperatures, the vapor pressure of tin is almost a full order of magnitude higher than that of copper. In addition to Cu-Sn alloys, a few Cu-Zn alloys were also prepared. Zinc boils at 907 °C, so one would expect far greater loss of zinc during processing, and this is also observed.

Table 1. Vapor Pressures of Metals at 1300 °C (Pa)

	Vapor Pressure (Pa)
Copper	3.1
Tin	21.2
Zinc	$>1.01*10^5$

Finally, an alloy of Cu-18.5 at% Sn was prepared. EDS measurements confirmed a final composition of the fibers to be Cu-15 at% Sn, the composition necessary for pseudoelasticity. Mechanically constrained thermal cycling, performed using a dynamic mechanical analyzer (DMA), shown in Figure 13, did not show any evidence of a martensitic phase transformation. Fibers were etched in 5% HF to see if there were any underlying structures responsible for the lack of apparent pseudoelasticity. In samples that were not annealed, Figure 14(a), it can clearly be seen that an oligocrystalline structure is present; that is, grain boundaries are nearly perpendicular to the wire axis. After annealing, however, two-phases become apparent. The compositions of these two phases align well with Figure 3(iii) on the phase diagram, though the samples were annealed in Region I.

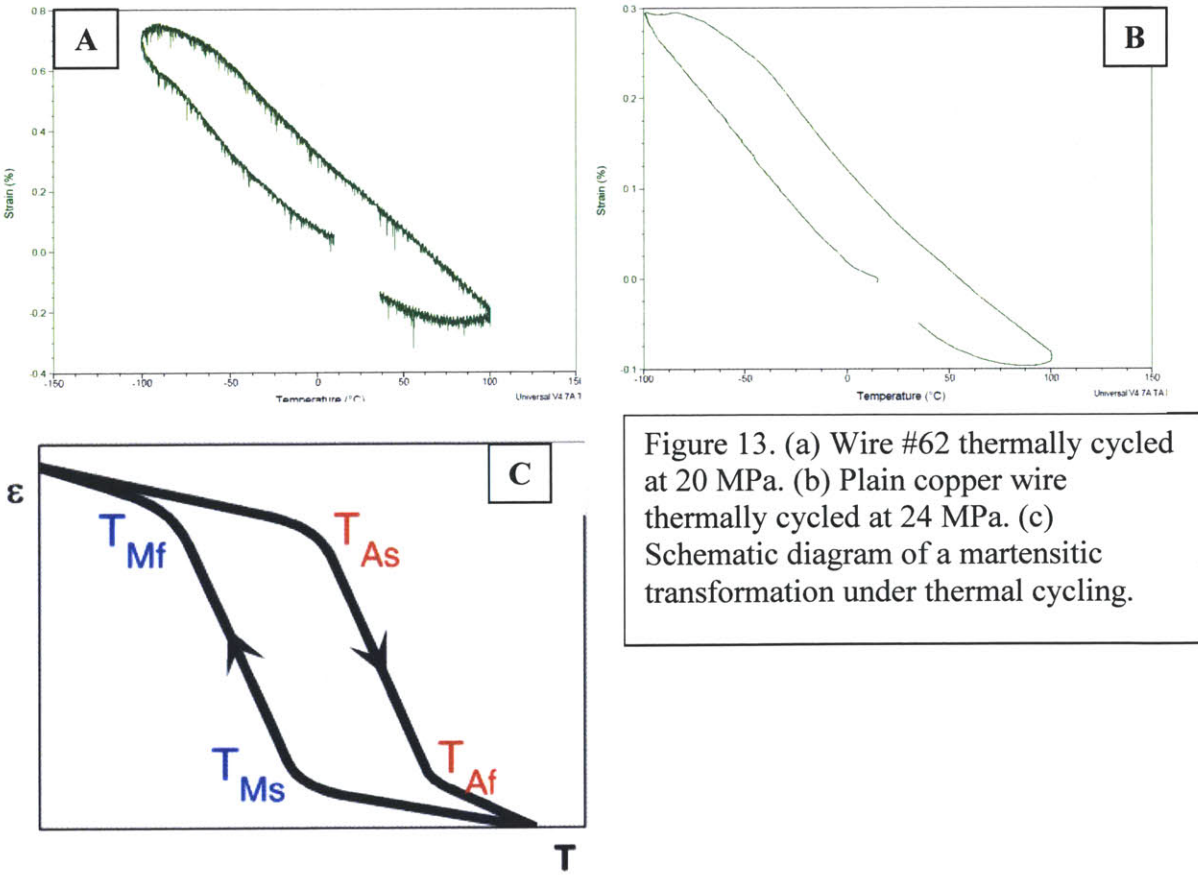

Figure 13. (a) Wire #62 thermally cycled at 20 MPa. (b) Plain copper wire thermally cycled at 24 MPa. (c) Schematic diagram of a martensitic transformation under thermal cycling.

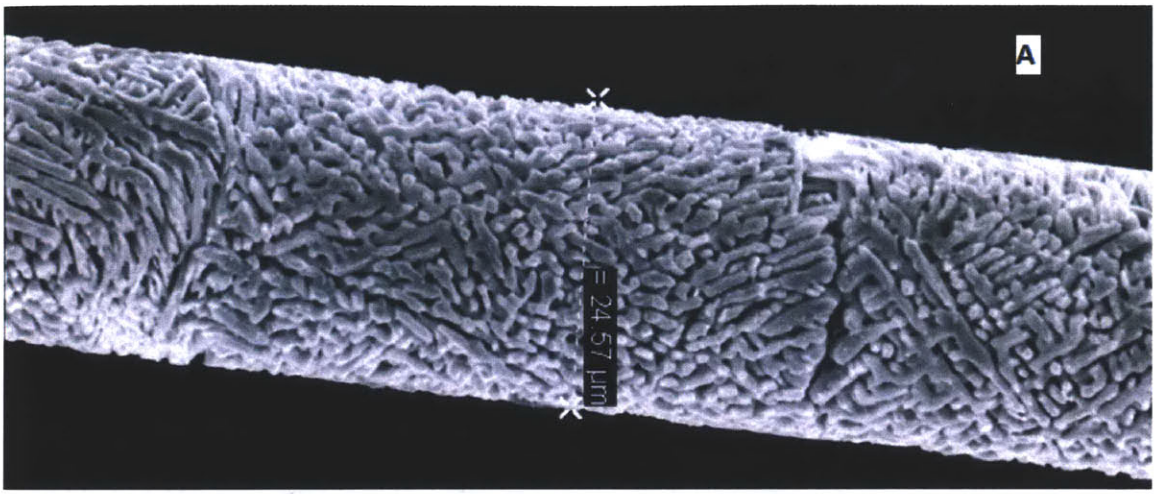

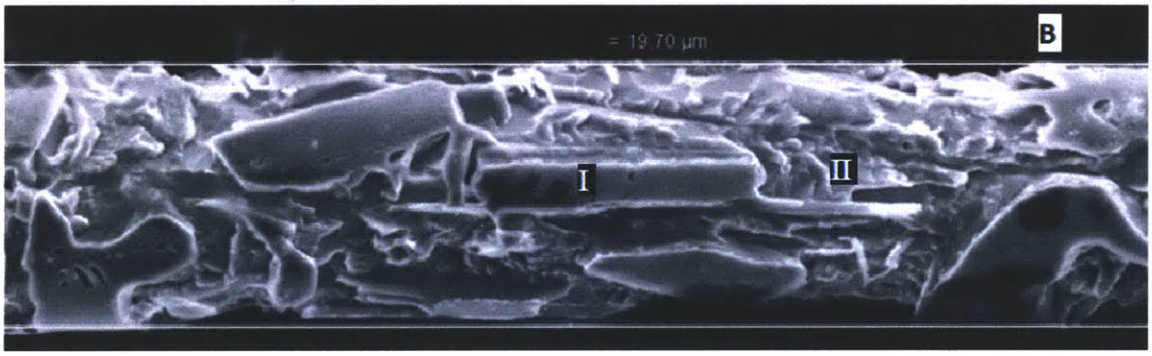

C

EDS Region I		
Copper	Tin	(at%)
88 %	12 %	

D

EDS Region II		
Copper	Tin	(at%)
82 %	18 %	

Figure 14. (a) Wire #61 not annealed and etched in 5% HF. (b) Wire #61 annealed for 15 minutes at 750 °C. (c-d) Quantitative EDS results of regions I & II

This difference in could most easily be explained by poor quenching. This explanation, however, is unlikely due to the fibers' small size, and the inability to get a single phase after multiple attempts. Another possible explanation is that this phase isn't stable at these length scales. The aging properties of this alloy have been studied numerous times [3, 7, 19, 37]. It has been confirmed that this alloy will even age at room temperature, greatly affecting the resulting shape memory properties [7, 19]. This may explain why we see phase separation and no martensitic transformation.

6. Other Observations:

As the main purpose of this project is to pave the use of a continuous-draw Taylor method for use with shape memory alloys, it would be remiss not to list potential problems this particular method has with regards to production and scalability. These problems are by no means insurmountable, however, they will have to be taken into account before industrial scale processing can truly be achieved.

6.1 Loss due to volatilization:

Table 1 lists the vapor pressure for relevant metals at 1300 °C. Zinc has a vapor pressure several orders of magnitude greater than that of copper. In fact, the boiling point of Zinc is 907 °C. This means that one would expect to lose more zinc than copper in the course of processing, and that is what happens. Table 2 shows compositions of alloys before and after being drawn as determined by EDS measurements. The amount of zinc in Cu-Zn alloys dropped by almost half. Though vapor pressures of Cu and Sn are much closer, there is also a measurable drop in Sn.

Table 2. Compositional changes in Cu-X (at %) alloys before and after being drawn. Accurate to within ± 1%

Element	Composition Before Draw	Composition After Draw
Zinc	40 %	24 %
Tin	14.5 %	10 %
Tin	17 %	14 %
Tin	18.5 %	15 %

This is important to account for because as mentioned previously SMAs are hugely dependent on composition. Changing the composition by even a few percent can change the transformation temperatures several hundred degrees [7, 19].

6.2 Density differences between metal and glass:

Copper, even in a liquid state, has a density higher than that of glass. The densities are 7.8 g/cm^3 and 2.23 g/cm^3 respectively. This means that while the metal is being drawn, it is also "falling" through the glass. This problem is not a major issue in the current setup, because the metal pellet being drawn is small (~.02 grams). When multiple pellets are drawn, the process always stops mid-way. A blackened, oxidized metal chunk is found extending beyond the tip of the glass. One potential solution to this problem would be to implement a metal-feeding system.

7. Conclusion:

A semi-automated Taylor method processing route was developed and refined. Cu-Sn and Cu-Zn microwires of up to 5 meters were drawn. These fibers were nearly continuous and uniform and varied between 10 – 35 microns in diameter. It was realized that process does not maintain perfect compositional purity. This problem, however, can be crudely overcome by simply adjusting the composition of the initial alloy. An SMA of Cu-15 at%Sn was studied in-depth and was determined to be a poor alloy for microwire production due to an apparently unavoidable phase separation. Finally, temperature and

draw speed and their effects on fiber diameter were studied. The draw speed varied over a range of 0.1 – 1 m/s fibers seems to have little effect on diameters. Composition of the alloy had no effect either. Temperature, however, can explain most of the variation in diameters seen in the microwires.

8. Future Work:

While this work takes some of the critical first steps toward the realization of industrial-scale production of shape memory micro-fibers, there is still much that needs to be done. The first, and foremost of these objectives would be to use the semi-automated Taylor machine to draw fibers that have shape memory properties by trying alternative alloys. Once that has been done, the fibers' properties can be tested to determine viability for commercial use. Furthermore, the technique to produce the fibers can be further automated and refined to draw fibers exceeding five meters in length. Finally, it would be interesting to know if properties can be enhanced if the fibers are incorporated into larger structures such as braids, cables, or textiles.

Appendix:

Table 3. Comprehensive list of microwires drawn using the semi-automated Taylor method described above

Number	Alloy (at%)	Fiber Diameter (micron)	Fiber & Glass Diameter (micron)	speed* (m/s)	Atmosphere	Temperature (°C)	Length (m)
1	Cu-15 Sn	37.6	98.1		air	1250 –1450°C	
2	Cu-15 Sn	18.2	47.8		air	1250 –1450°C	
3	Cu-15 Sn	31.3	53.6	0.93	air	1250 –1450°C	
4	Cu-15 Sn	20.1	29.6	0.91	air	1250 –1450°C	
5	Cu-15 Sn	15.6	35.9	0.78	air	1250 –1450°C	
6	Cu-15 Sn	152.5	293.5		air	1250 –1450°C	
7	Cu-15 Sn	20.5	40.9		air	1250 –1450°C	
8	Cu-15 Sn	33.7	71.6		air	1250 –1450°C	
9	Cu-15 Sn	11.0	22.9		air	1250 –1450°C	
10	Cu-15 Sn	11.5	18.4		air	1250 –1450°C	
11	Cu-39 Zn	36.2	66.9		air	1250 –1450°C	
12	Cu-39 Zn	13.6	29.2	0.99	air	1250 –1450°C	
13	Cu-39 Zn	18.9	29.5	0.99	air	1250 –1450°C	
14	Cu-39 Zn	9.0	50.6	0.95	air	1250 –1450°C	
15	Cu-39 Zn	25.7	49.6	0.90	air	1250 –1450°C	
16	Cu-39 Zn	20.9	48.0	0.90	air	1250 –1450°C	
17	Cu-39 Zn	32.3	68.3	0.48	air	1250 –1450°C	
18	Cu-39 Zn	84.2	138.3	0.19	air	1250 –1450°C	
19	Cu-39 Zn	18.6	33.5	0.19	air	1250 –1450°C	
20	Cu-39 Zn	13.6	24.9	0.32	air	1250 –1450°C	
21	Cu-39 Zn	22.9	55.7	0.32	air	1250 –1450°C	
22	Cu-39 Zn	31.1	59.4		air	1250 –1450°C	
23	Cu-39 Zn	18.7	47.7		air	1250 –1450°C	
24	Cu-39 Zn	15.7	29.1	0.42	air	1250 –1450°C	
25	Cu-39 Zn	20.6	47.7		air	1250 –1450°C	
26	Cu-39 Zn	31.5	61.1	0.43	air	1250 –1450°C	
27	Cu-39 Zn	15.6	92.4		air	1250 –1450°C	
28	Cu-14.5 Sn	15.7	28.7	0.83	air	1250 –1450°C	
29	Cu-14.5 Sn	12.3	31.0	0.64	air	1250 –1450°C	
30	Cu-14.5 Sn	29.6	48.6	0.40	air	1250 –1450°C	
31	Cu-14.5	18.2	26.0	0.64	air	1250 –1450°C	

	Sn						
32	Cu-14.5 Sn	23.9	49.4	0.64	air	1250 –1450°C	
33	Cu-14.5 Sn	17.8	25.4	0.64	air	1250 –1450°C	
34	Cu-14.5 Sn	20.3	57.5	0.62	air	1250 –1450°C	
35	Cu-14.5 Sn	21.9	68.1	0.45	air	1250 –1450°C	
36	Cu-40 Zn	9.5	36.6	0.53	air	1250 –1450°C	
37	Cu-40 Zn	16.9	31.2	0.53	air	1250 –1450°C	1.74
38	Cu-40 Zn	16.7	35.5	0.71	air	1250 –1450°C	3.32
39	Cu-40 Zn	22.6	30.3	0.71	air	1250 –1450°C	
40	Cu-40 Zn	13.2	35.5	0.86	air	1250 –1450°C	3.22
41	Cu-40 Zn	16.9	45.2	0.86	air	1250 –1450°C	
42	Cu-26 Sn	13.0	33.0		air	1250 –1450°C	
43	Cu-26Sn	17.7	32.4	0.78	air	1250 –1450°C	
44	Cu-26Sn	11.8	24.9	0.64	air	1250 –1450°C	
45	Cu-26Sn	14.0	30.8	0.88	air	1250 –1450°C	
46	Cu-26Sn	19.2	27.9	0.48	air	1250 –1450°C	
47	Cu-17Sn	21.2	41.2	0.23	air	1250 –1450°C	
48	Cu-17Sn	18.9	29.2	0.42	air	1250 –1450°C	
49	Cu-17Sn	16.3	32.5	0.42	air	1250 –1450°C	
50	Cu-17Sn	17.0	35.7	0.33	air	1250 –1450°C	
51	Cu-18.5Sn	13.0		0.42	air	1250 –1450°C	
52	Cu-18.5Sn	16.6	32.9	0.33	air	1250 –1450°C	
53	Cu-18.5Sn	12.8			air	1250 –1450°C	
54	Cu-18.5Sn	14.4	21.2		air	1250 –1450°C	
55	Cu-18.5Sn	37.6	62.4		air	1250 –1450°C	
56	Cu-18.5Sn	29.6	48.4	0.33	air	1250 –1450°C	
57	Cu-18.5Sn	42.4	59.3	0.33	air	1250 –1450°C	
58	Cu-18.5Sn	15.2	24.5	0.33	air	1250 –1450°C	
59	Cu-18.5Sn	13.6	20.0	0.33	air	1250 –1450°C	
60	Cu-18.5Sn	17.8	26.6	0.33	air	1250 –1450°C	
61	Cu-	29.0	52.0	0.33	air	1250 –1450°C	

	18.5Sn						
62	Cu-18.5Sn	13.6	24.3	0.32	argon	1400	
63	Cu-18.5Sn	16.6	30.3	0.32	argon	1350	2.0
64	Cu-18.5Sn	13.0	31.9	0.64	argon	1382.5	3.7
65	Cu-17Sn	22.2	35.9	0.32	argon	1385	4.8
66	Cu-17Sn	7.4	15.4	0.32	argon	1417.5	4.6
67	Cu-17Sn	12.7	20.6	0.90	argon	1415	4.6
68	Cu-17Sn	28.0	56.5	0.32	argon	1345	
69	Cu-17Sn	51.6	94.8	0.32	argon	1400	
70	Cu-17Sn	13.5	30.5	0.32	argon	1380	

* Speed values not listed were drawn by hand

References:

[1] Chen Y, Schuh C, *Size effects in shape memory alloy microwires,* Acta Mater, **59**, 537 (2011)

[2] Ueland S, Schuh C, *Superelasticity and fatigue in oligocrystalline shape memory alloy microwires,* Acta Mater, **60**, 282 (2012)

[3] Kato H, Hirata N, Miura, *Effects of aging on pseudoelastic behavior in Cu-15.0at% Sn Alloy Single Crystals,* Acta Mater, **43**, 361 (1995)

[4] Sutou Y, et. al., *Development of medical guide wire of Cu-Al-Mn-Base superelastic alloy with functionally graded characteristics,* J Biomed Mater Res Part B, **69B**, 64 (2004)

[5] Kohl M, et. al., *Powder metallurgical near-net-shape fabrication of porous NiTi shape memory alloys..,* Adv Eng Mater, **11**, 959 (2009)

[6] Schroeder T, Wayman C, *The formation of martensite and the mechanism of the shape memory effect in single crystals of Cu-Zn alloys*, Acta Metal, **25**, 1375 (1977)

[7] Miura S, Maeda S, Nakanishi N, *Pseudoelastic and shape memory phenomena related to stress-induced martensite in Cu-15.0 at%Sn alloy,* Scrip Meta, **9**, 675 (1975)

[8] Huan Z, Fratila-Apachitei L, Apachitei I, Duszczyk J, *Porous NiTi surfaces for biomedical applications*, Applied Surface Science, **258,** 5244 (2012)

[9] Biesiekierski A, Wang J, Gepreel M, Wen C, *A new look at biomedical Ti-based shape memory alloys*, Acta Biomater, **8,** 1661 (2012)

[10] Lagoudas, Dimitris C. *Shape Memory Alloys: Modeling and Engineering Applications*. New York: Springer (2008)

[11] Funakubo, Hiroyasu, ed. *Shape Memory Alloys*. New York: Gordon and Breach Science (1987)

[12] Bertolino G, et. al., *Mechanical properties of martensitic Cu-Zn-Al foams in the pseudoelastic regime,* Mat. Lett., **64**, 1448 (2010)

[13] San Juan J, Nó M, Schuh C, *Nanoscale shape-memory alloys for ultrahigh mechanical damping,* **4**, 415 (2009)

[14] Holschuh, Brad. Dept Aero and Astro. *PhD Thesis Proposal.* MIT (2011)

[15] Recarte V, Perez-Saez R, Bocanegra E, Nó M, San Juan J, *Influence of Al and Ni concentration on the martensitic transformation in Cu-Al-Ni shape-memory alloys*, Meta and Mater Trans, **33A**, 2581 (2002)

[16] Vives E, et. al., *Temperature contour maps at the strain-induced martensitic transition of a Cu-Zn-Al shape memory single crystal,* App Phys Lett, **98** (2011)

[17] Niitsu K, Omori T, Kainuma R, *Superelasticity at low temperatures in Cu-17Al-15Mn shape memory alloy,* Mater Trans, **52**, 1713 (2011)

[18] Ahlers M, *Martensite and equilibrium phases in Cu-Zn and Cu-Zn-Al alloys*, Prog Mater Sci, **30**, 135 (1986)

[19] Castro Riglos M, Pelegrina J, Ahlers, *Phase stability in Cu-Zn-basted ternary alloys with elements of column 14*, Mater Sci & Eng A, **481**, 504 (2008)

[20] Yausa M, Kajikawa K, Hakamada M, Mabuchi M, *A superelastic nanocrystalline Cu-Sn alloy thin film processed by electroplating,* Mater Letters, **62**, 4473 (2008)

[21] Stice J, Wayman CM, *Observations of aging effects in a Cu-Sn Shape Memory Alloy*, Meta Trans, **13A**, 1687 (1982)
[22] Kato H, Sasaki K, *Avoiding error of determining the martensitic finish temperature due to thermal inertia in differential scanning calorimetry: model and experiment of Ni-Ti and Cu-Al-Ni shape memory alloys,* J Mater Sci, **47**, 1399 (2012)
[23] Colic M, et. al., *Relationship between microstructure, cytotoxicity, and corrosion properties of a Cu-Al-Ni shape memory alloy*, Acta Biomater, **6**, 308 (2010)
[24] Taylor G, *A method of drawing metallic filaments and a discussion of their properties and uses,* Fine Metallic Filaments 655 (1924)
[25] Donald I, *Review: production, properties and applications of microwire and related products,* J of Mat Sci, **22,** 2661 (1987)
[26] Donald I, Metcalfe B, *The preparation, properties and applications of some glass-coated metal filaments prepared by the Taylor-wire process,* J. of Mat. Sci, **31**, 1139 (1996)
[27] Manfre G, Servi G, Ruffino C, *Copper microwires spun from the melt*, J. of Mat. Sci, **9,** 74 (1974)
[28] Larin V, et.al., *Preparation and properties of glass-coated microwires*, J. of Mag. and Mag. Mat. **249,** 39 (2002)
[29] Pardoe, G, Butler E, Gelder D, *Rapid quenching by the Taylor wire technique,* J. of Mat Sci, **13,** 786 (1978)
[30] Goto T, *The preparation of fine Ni-Fe-base amorphous filaments using the method of glass coated melt spinning*, Mat Sci and Eng, **59,** 251 (1983)
[31] Ochin P, et. al., *Shape memory thin round wires produced by the in rotating water melt spinning technique*, Acta Mater, **54,** 1877 (2006)
[32] Craciunescu C, et. al., *Rapidly solidified ferromagnetic shape memory alloys,* Eur Phys J Spec Topics, **158,** 161 (2008)
[33] Han K, Embury J, Petrovic J, Weatherly G, *Microstructural aspects of Cu-Ag produced by the Taylor wire method*, Acta Meta, **46,** 4691 (1998)
[34] Baikov A, French Patent 1361929 (1963)
[35] McKenica W, US Patent 3214805 (1965)
[36] Irisawa T, Cargill G, Hwang K, Maniatty A, *Viscous elongation of glass rods: experiments, simulations, and analysis*, J App Phys, **108**, 113515 (2010)
[37] Kuwano N, Wayman CM, *Microstructural Changes in an Aged Cu-15 at%Sn Shape Memory Alloys*, Trans Japan Inst of Metals, **24,** 504 (1983)